Slow-light solitons in coupled asymmetric quantum wells via interband transitions

Chengjie Zhu[1] and Guoxiang Huang[2,3,*]

[1]*Department of Physics, East China Normal University, Shanghai 200062, China*
[2]*State Key Laboratory of Precision Spectroscopy, Department of Physics, East China Normal University, Shanghai 200062, China*
[3]*Institute of Nonlinear Physics, Department of Physics, Zhejiang Normal University, Zhejiang 321004, China*

We investigate the formation and propagation of optical solitons in an asymmetric double quantum-well structure. Using a standard method of multiple scales we derive a nonlinear Schrödinger (NLS) equation with some high-order correction terms that describe effects of linear and differential absorption, nonlinear dispersion, delay response of nonlinear refractive index, and third-order dispersion of a probe field. We show that in order to make slowly varying envelope approximation be valid an excitation scheme of interband transition should be adopted. We also show that for realistic quantum-well parameters the probe field with time length of picosecond or shorter must be used to make dispersion and nonlinear lengths of the system be smaller than absorption length, only by which a shape-preserving propagation of optical solitons is available. In addition, we clarify validity domains for the perturbed NLS equation as well as the high-order NLS equation and provide various optical soliton solutions in different regimes both analytically and numerically. We demonstrate that the solitons obtained have ultraslow propagating velocity and can be generated under very low input light intensity.

I. INTRODUCTION

In recent years, much attention has been paid to the study of optical solitons due to their important applications for optical information processing and transmission.[1] However, most optical solitons realized up to now are produced in passive media such as glass-based optical fibers in which far-off resonance excitation schemes are used for avoiding serious optical absorption. Because nonlinear effect in passive media is extremely weak, for producing optical solitons high-input light intensity and long propagation distance are required. In addition, optical solitons generated in this way generally travel with a speed very close to c, the light speed in vacuum.[2]

The basic mechanism for the formation of temporal optical soliton is the balance between nonlinearity and dispersion. For reducing the formation distance of the soliton and changing its propagating velocity far from c, a material with large dispersion and Kerr nonlinearity is needed. It is well known that Kerr nonlinearity and group-velocity dispersion can be enhanced greatly if a system works near resonance. In fact, in the early days of nonlinear optics there were substantial efforts in utilizing resonant atomic systems to realize efficient nonlinear optical processes. Unfortunately, resonance enhancement of nonlinearity and dispersion usually accompany with a strong absorption. For this reason, it was generally recognized that even though large nonlinearity and dispersion can be obtained in resonant media, it is practically difficult to take advantages of such resonance enhancement. However, in recent years such paradigm has been challenged by the study of electromagnetically induced transparency (EIT) in resonant atomic systems.[3] Due to the quantum interference effect induced by a control field, the propagation of a weak probe field has many striking features, including large suppression of optical absorption, significant reduction in probe-field group velocity, and giant enhancement of Kerr nonlinearity.[3] Based on these important features, it has been

suggested recently that a new type of optical solitons, i.e., *ultraslow optical solitons*, are possible in highly resonant atomic systems.[4–9]

On the other hand, in recent years there have been a lot of efforts on similar quantum interference effects in semiconductors. One of important motivations of such study comes from the drastic increase in applications because of the widespread use of semiconductor components in optoelectronics and quantum information science. Quantum coherent phenomena (e.g., lasing without inversion, coherent population oscillations, EIT, and slow light, etc.) in semiconductor heterostructures have been explored both theoretically and experimentally.[10–25] Specifically, Fano interference in asymmetric double quantum wells and related phenomenon of tunneling-induced transparency (TIT) via intersubband transitions have been intensively investigated.[26–33] It has also been suggested that enhanced Kerr nonlinearity, all optical switching, four-wave mixing, and slow optical solitons are possible in such systems.[34–40]

In this work, we investigate the dynamics of optical solitons in an asymmetric double quantum-well structure. We shall show that, for realistic quantum-well parameters and to make slowly varying envelope approximation (SVEA) be valid, an excitation scheme with interband transitions must be adopted, which is different from Refs. 40 and 41, where an intersubband transition scheme was used. Furthermore, we shall show that the probe field with time length of picosecond or even shorter must be used to make dispersion and nonlinear lengths less than absorption length, only under such condition a shape-preserving propagation of an optical soliton is available. Different from EIT-based atomic systems, where the probe pulse has time length generally around microsecond[4–9] and hence nonlinear and dispersion effects are comparably weak, the optical soliton in the quantum-well system have much shorter time length and thus the nonlinear and dispersion effects are much stronger. Hence it is very necessary to consider how high-order dispersion and high-order nonlinear effects affect the property and dynamics of
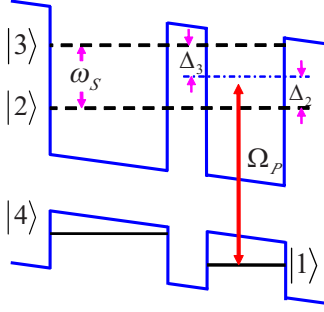
FIG. 1. (Color online) Energy-level diagram and excitation scheme of the asymmetric double quantum-well structure. $|2\rangle$ and $|3\rangle$ are delocalized bonding and antibonding electronic states of conduction band arising from tunneling effect. $|1\rangle$ and $|4\rangle$ are localized hole states of valence band. Ω_p is the half Rabi frequency of the probe field, Δ_2 and Δ_3 are detuning, and ω_s is the energy interval between the state $|2\rangle$ and the state $|3\rangle$.

the optical soliton in the quantum-well system. By using a standard method of multiple scales we derive a nonlinear Schrödinger (NLS) equation with high-order correction terms that describe effects of linear and differential absorption, nonlinear dispersion, delay response of nonlinear refractive index, and third-order dispersion of the probe field. We shall demonstrate that the high-order correction terms take indeed a significant role when the probe pulse duration is just less than one picosecond and provide various optical soliton solutions that have ultraslow propagating velocity and very low generation power.

The paper is arranged as follows. In Sec. II, we present the theoretical model of the coupled double quantum well and discuss its solution in linear regime. In Sec. III, we give a detailed derivation of a high-order NLS equation describing the evolution of the probe field. In Sec. IV, we give various soliton solutions both analytically and numerically and discuss their formation and propagation dynamics. A summary of main results obtained in this work is given in the last section.

II. MODEL AND ITS SOLUTION IN LINEAR REGIME

The asymmetric couple quantum-well structure we consider is the same as that in Ref. 42, which consists of a narrow well and a wide well, separated by a narrow barrier, as shown in Fig. 1. In such quantum-well system, the first electron level in conduction band of the wide well can be energetically aligned with the first electron level of the narrow well by applying a static electric field with a given polarity, whereas the first hole levels in valence band of both the wide and narrow wells are never aligned for this polarity of the static electric field (for detail, see Ref. 42). Thus electrons will delocalize and the levels will split into a bonding and an antibonding states arising from tunneling effect, labeled $|2\rangle$ and $|3\rangle$, respectively. The holes remain localized, which correspond to $|1\rangle$ and $|4\rangle$. The splitting ω_s between $|2\rangle$ and $|3\rangle$ can be controlled by adjusting the height and width of the tunneling barrier with applied bias voltage. As in Refs. 35–41, we assume (i) the system works in low-temperature

environment [e.g., in a continuous-flow cryostat at temperature of 10 K (Ref. 42)] and the carrier density in the wells is low enough, and (ii) the difference between effective masses in different subbands is small. The latter condition is, strictly speaking, valid only for the situation when the subbands are parallel and Coulomb and Fröhlich matrix elements have a two-dimensional character. In this case, the quantized electron motion perpendicular to layers in growth direction of the wells is decoupled from the free motion in the quantum-well plane, and intrasubband electron-electron and electron-phonon interactions do not affect intersubband coherence (for detail, see Ref. 43). Making such assumptions is for sake of simplicity for theoretical analysis and we believe that these effects are of significance only in final engineering optimization without changing basic physical property under study.[33]

A weak probe optical pulse with angular frequency ω_p, wave number $k_p = \omega_p/c$, polarization vector $\mathbf{e}_p$, and amplitude E_p is assumed to propagate in z direction and interacts with such four-level system. The probe pulse induces the transitions $|1\rangle \leftrightarrow |2\rangle$ and $|1\rangle \leftrightarrow |3\rangle$ with the respective half Rabi frequencies $(\boldsymbol{\mu}_{21} \cdot \mathbf{e}_p) E_p/\hbar$ and $(\boldsymbol{\mu}_{31} \cdot \mathbf{e}_p) E_p/\hbar$, where $\boldsymbol{\mu}_{31}$, $\boldsymbol{\mu}_{21}$ are corresponding interband dipole moments. Detunings are defined by $\Delta_2 = \omega_p - (E_2 - E_1)/\hbar$ and $\Delta_3 = (E_3 - E_1)/\hbar - \omega_p$, where E_j is the eigenenergy of the state $|j\rangle$. Using the energy splitting $\omega_s = (E_3 - E_2)/\hbar$, we can express the detunings as $\Delta_2 = \omega_s/2 + \delta$ and $\Delta_3 = \omega_s/2 - \delta$, where $\delta = \omega_p - (E_2 + E_3 - 2E_1)/(2\hbar)$. Under electric dipole and rotating-wave approximations, the equations of motions controlling the evolution of the probability amplitudes A_j of the state $|j\rangle$ ($j = 1-3$) are

$$i\frac{\partial}{\partial t}A_1 + \Omega_p^* A_2 + g_1^* \Omega_p^* A_3 = 0, \tag{1a}$$

$$\left(i\frac{\partial}{\partial t} + d_2\right)A_2 + \Omega_p A_1 - i\kappa A_3 = 0, \tag{1b}$$

$$\left(i\frac{\partial}{\partial t} + d_3\right)A_3 + g_1\Omega_p A_1 - i\kappa A_2 = 0 \tag{1c}$$

with $g_1 = \mu_{31}/\mu_{21}$, $d_2 = \Delta_2 + i\gamma_2$, $d_3 = -\Delta_3 + i\gamma_3$, and $\Omega_p \equiv (\boldsymbol{\mu}_{21} \cdot \mathbf{e}_p) E_p/(\hbar)$. Here total decay rate γ_j of the state $|j\rangle$ consists of population decay rate γ_{jl}, primarily due to longitudinal-optical-phonon emission events at low temperature, and dephasing rates γ_j^{dph}, determined by electron-electron scattering, interface roughness and phonon-scattering processes, i.e., $\gamma_j = \gamma_{jl} + \gamma_j^{\text{dph}}$. The population decay rate γ_{jl} can be calculated by solving effective-mass Schrödinger equation. For the temperatures up to 10 K, the electric density kept below 5×10^{11} cm^{-2} per double well to minimize dephasing from carrier scattering, the dephasing decay rate γ_j^{dph} can be estimated according to experiments.[44] In Eqs. (1b) and (1c), the parameter $\kappa = \sqrt{\gamma_{2l}\gamma_{3l}}$ denotes the cross coupling of states $|2\rangle$ and $|3\rangle$ via the longitudinal-optical-phonon decay, describing the process in which a phonon is emitted by subband $|2\rangle$ and recaptured by subband $|3\rangle$.[45,46]

The evolution of the probe field is governed by the Maxwell equation $\nabla^2 \mathbf{E} - (1/c^2)\partial^2 \mathbf{E}/\partial t^2 = (1/\epsilon_0 c^2)\partial^2 \mathbf{P}/\partial t^2$, where $\mathbf{P} = N[\boldsymbol{\mu}_{31}A_1A_3^* \exp(k_p z - \omega_p t) + \boldsymbol{\mu}_{21}A_1A_2^* \exp(k_p z - \omega_p t) + \text{c.c.}]$. For simplicity, we assume that the probe field is homogeneous in the transverse (i.e., x and y) directions. Then under the SVEA, i.e.,

$$\frac{\partial \Omega_p}{\partial z} \ll k_p \Omega_p, \tag{2a}$$

$$\frac{\partial \Omega_p}{\partial t} \ll \omega_p \Omega_p, \tag{2b}$$

the Maxwell equation is reduced to

$$i\left(\frac{\partial}{\partial z} + \frac{1}{c}\frac{\partial}{\partial t}\right)\Omega_p + B(A_2 + g_1^* A_3)A_1^* = 0, \tag{3}$$

where $B = N\omega_p|\boldsymbol{\mu}_{21}|^2/2\hbar\epsilon_0 c$ with N being the electron density in the valence band of the quantum well.

We first look at the eigensolutions of Eqs. (1a)–(1c) by assuming that the probability amplitudes A_j follow the variation in Ω_p. Writing Eqs. (1a)–(1c) as $i\hbar \partial A/\partial t = \hat{H}A$ with $A = (A_1, A_2, A_3)^T$ and $\hat{H} = \hbar[(d_2|2\rangle\langle 2| + d_3|3\rangle\langle 3| + \Omega_p|2\rangle\langle 1| + g_1\Omega_p|3\rangle\langle 1| + \text{c.c.}) - i\kappa|3\rangle\langle 2| - i\kappa|2\rangle\langle 3|]$. Under the conditions $|g_1| = 1$, $\gamma_j \approx \gamma_j^{\text{dph}}$, and $\gamma_2 \approx \gamma_3$, one can obtain the eigenvalues of $\hat{H}$ as $\lambda_1 \approx 0$, $\lambda_2 = i\gamma_2 + \frac{1}{2}(\omega_s^2 + 8|\Omega_p|^2 - 4\gamma_2^2)^{1/2}$, $\lambda_3 = i\gamma_2 - \frac{1}{2}(\omega_s^2 + 8|\Omega_p|^2 - 4\gamma_2^2)^{1/2}$. Because both λ_2 and λ_3 are complex, the corresponding eigenmodes attenuate rapidly. These modes are not interesting for wave-propagation problem and hence will not be considered further. However, the zero mode (the eigenmode with $\lambda_1 \approx 0$) has a vanishing decay and thus is important. It is easy to get the eigenvector of the zero mode, which reads $\{1/(1 + 8|\Omega_p|^2/\omega_s^2)^{1/2}, -2\Omega_p/[\omega_s(1 + 8|\Omega_p|^2/\omega_s^2)^{1/2}]$, and $-2\Omega_p/[\omega_s(1 + 8|\Omega_p|^2/\omega_s^2)^{1/2}]\}$. Obviously, if $\omega_s \gg \Omega_p$, nearly all electrons remain in the energy level $|1\rangle$ and the population in energy levels $|2\rangle$ and $|3\rangle$ is negligible, i.e., $(A_1, A_2, A_3) \approx (1, 0, 0)$. In this case the probe field does not feel the existence of energy levels $|2\rangle$ and $|3\rangle$ and hence it can propagate transparently in the system. Thus the zero-mode state of the system is similar to the dark state in resonant atomic systems with EIT.[3] However, the formation mechanism of the dark state here is different from that of EIT since it results from a tunneling effect that induces the mixing of the electronic levels between the wide and narrow wells.

Before exploring weak nonlinear effects, it is necessary to examine the linear property of the system. To this aim we assume electrons are initially populated the energy level $|1\rangle$ and the probe-field intensity is very small. In this situation the population of the ground state $|1\rangle$ is not depleted during time evolution, i.e., $A_1 \approx 1$. Taking A_2 and A_3, and Ω_p to be proportional to $\exp[i(Kz - \omega t)]$, by the Maxwell-Schrödinger Eqs. (1a)–(1c), (2a), (2b), and (3) we obtain the linear-dispersion relation of the system
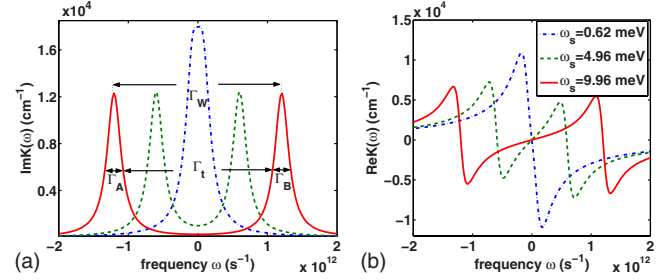

FIG. 2. (Color online) Linear-dispersion relation as functions of ω. Panels (a) and (b) are curves of Im $K(\omega)$ and Re $K(\omega)$ characterizing linear absorption and refractive index, respectively. The doted, dashed, and solid lines in the figure correspond to $\omega_s = 0.62$, 4.96, and 9.96 meV, respectively. The other parameters are given in the text. The definition of the transparency-window width Γ_w, transmission width Γ_t, and absorption linewidth $\Gamma_{A(B)}$ are given in the figure.

$$K(\omega) = \frac{\omega}{c} - B\frac{(\omega + d_3) + |g_1|^2(\omega + d_2) + i(g_1 + g_1^*)\kappa}{D} \tag{4}$$

with $D \equiv (\omega + d_2)(\omega + d_3) + \kappa^2$. In most cases, $K(\omega)$ can be Taylor expanded around the center frequency of the probe field, which corresponds to $\omega = 0$, i.e., $K(\omega) = K_0 + K_1\omega + (K_2/2)\omega^2 + \cdots$, where $K_j = (\partial^j K/\partial\omega^j)|_{\omega=0}$ with $1/K_1$ representing a complex group velocity, and K_2 the group-velocity dispersion and additional loss of the probe field.

Shown in Figs. 2(a) and 2(b) are the imaginary part Im $K(\omega)$ and the real part Re $K(\omega)$ of the linear-dispersion relation, respectively. The dot-dashed, dashed, and solid lines in the figure are the results for $\omega_s = 0.62$ meV (1.51×10^{11} s^{-1}), 4.96 meV (1.2×10^{12} s^{-1}), and 9.96 meV (2.41×10^{12} s^{-1}), respectively. Parameters we chosen are suitable to a typical double quantum-well structure,[42] which has a 51-monolayer (ML) (145 Å) wide well and a 35-monolayer (100 Å) narrow well, separated by an 9-monolayer (26 Å) Al$_{0.2}$Ga$_{0.8}$As buffer layer at the temperature of 10 K, with $|g_1| = 1.0$ and $B = 6.2 \times 10^5$ m^{-1} meV. Population decay rates and the dephasing rates of the subbands $|2\rangle$ and $|3\rangle$ can be estimated according to Refs. 38 and 47. One can choose $\gamma_{2l} = 1.28$ ns^{-1}, $\gamma_{3l} = 1.29$ ns^{-1}, $\gamma_2^{\text{dph}} = \frac{1}{8}$ ps^{-1}, $\gamma_3^{\text{dph}} = \frac{1}{8}$ ps^{-1}, and ω_s can be controlled by adjusting the height and width of the tunneling barrier experimentally.

From Fig. 2(a) we see that for small ω_s the absorption profile has only a single peak, hence the probe field with the central angular frequency ω_p (corresponding to $\omega = 0$) is largely absorbed. However, if increasing ω_s to make ω_s^2 be much larger than $4\gamma_2\gamma_3$, the absorption profile displays a large Autler-Townes absorption doublet (i.e., TIT transparency window). For characterizing the absorption doublet, we define TIT window width Γ_w (i.e., the distance between the maxima of the two absorption peaks of the doublet), the transmission width Γ_t (i.e., the minimum distance between two absorption peaks at half maxima), and the absorption linewidth Γ_A (Γ_B) which is the width of the absorption line A (B), as shown in Fig. 2(a). From the linear-dispersion relation (4) and under the conditions $\gamma_2 \simeq \gamma_3 \simeq \kappa$, and $g_1 \simeq -1$, we obtain the following explicit expressions

$$\Gamma_w = \frac{2\gamma_2\sqrt{\omega_s^2 + 16\gamma_2^2} + \sqrt{\omega_s^4 - 12\omega_s^2\gamma_2^2 + 64\gamma_2^4}}{\sqrt{\omega_s^2 - 16\gamma_2^2}}, \quad (5a)$$

$$\Gamma_t = \frac{-2\gamma_2\sqrt{\omega_s^2 + 16\gamma_2^2} + \sqrt{\omega_s^4 - 12\omega_s^2\gamma_2^2 + 64\gamma_2^4}}{\sqrt{\omega_s^2 - 16\gamma_2^2}}, \quad (5b)$$

$$\Gamma_A \simeq \Gamma_B = \frac{2\gamma_2\sqrt{\omega_s^2 + 16\gamma_2^2}}{\sqrt{\omega_s^2 - 16\gamma_2^2}}. \quad (5c)$$

Obviously if $\omega_s \gg \gamma_2$, we have $\Gamma_w \simeq \Gamma_t \simeq \omega_s$. Thus, the larger the tunneling coupling ω_s, the larger the TIT transparency window.

In addition to the appearance of the Autler-Townes doublet in the absorption profile, the dispersion part that corresponds to the linear refractive index [i.e., Re $K(\omega)$] also has a drastic variation for the change in ω_s. From Fig. 2(b) we see that when ω_s increases, the system is changed from an anomalous dispersion regime to a normal dispersion regime, and hence the sign of group velocity of the probe field, i.e., $V_g \equiv \partial \text{Re } K(\omega)/\partial\omega$, is changed from negative to positive. In the TIT transparency window, V_g is positive and can be very small.

III. ASYMPTOTIC EXPANSION AND HIGH-ORDER NLS EQUATION

We now turn to consider weak nonlinear excitations of the system. Our aim is to get a nonlinear probe pulse that allows shape-preserving propagation. Notice that, different from the EIT in atomic systems where dispersion and Kerr nonlinearity vanish at exact two-photon resonance,[3] in the present TIT system dispersion always exists because the detunings Δ_2 and Δ_3 cannot equal to zero simultaneously. Furthermore, for a large-amplitude probe field the Kerr nonlinearity is also significant. Thus we can use the balance between the dispersion and Kerr nonlinear effects to obtain a solitonlike nonlinear probe pulse. For this aim we use a standard method of multiple scales[5] to analyze the nonlinearly coupled Maxwell-Bloch Eqs. (1) and (3). We introduce the asymptotic expansion $A_j = \sum_{n=0}^{\infty} \varepsilon^n A_j^{(n)}$, $\Omega_p = \sum_{n=1}^{\infty} \varepsilon^n \Omega_p^{(n)}$ with $A_1^{(0)} = 1$, $A_2^{(0)} = A_3^{(0)} = 0$, here ε is a small parameter characterizing the small depletion of the ground state and $A_j^{(n)}$ and $\Omega_p^{(n)}$ ($n = 1, 2, \dots$) are functions of the multiscale variables $z_l = \varepsilon^l z$ ($l = 0$–3), $t_l = \varepsilon^l t$ ($l = 0, 1$). Substituting these expansions into Eqs. (1) and (3) one obtains a set of linear but inhomogeneous equations of $A_j^{(n)}$ and $\Omega_p^{(n)}$, which can be solved order by order.

The leading order ($n = 1$) reads

$$\Omega_p^{(1)} = Fe^{i\theta}, \quad (6a)$$

$$A_2^{(1)} = -\frac{(\omega + d_3) + ig_1\kappa}{D}Fe^{i\theta}, \quad (6b)$$

$$A_3^{(1)} = -\frac{g_1(\omega + d_2) + i\kappa}{D}Fe^{i\theta}, \quad (6c)$$

where $\theta = K(\omega)z_0 - \omega t$ and F is a yet to be determined envelope function depending on the slow variables x_1, y_1, t_1, and

z_j ($j = 1, 2, 3$). The dispersion function $K(\omega)$ is given by Eq. (4).

At the second order ($n = 2$), a condition of eliminating a secular term requires

$$i\left(\frac{\partial F}{\partial z_1} + \frac{1}{V_g}\frac{\partial F}{\partial t_1}\right) = 0. \quad (7)$$

The second-order solution is given by

$$A_1^{(2)} = -\frac{1}{2}\left[\frac{|\omega + d_3 + i\kappa g_1|^2 + |g_1(\omega + d_2) + i\kappa|^2}{|D|^2}\right]|F|^2 e^{-\bar{\alpha}z_2}, \quad (8a)$$

$$A_2^{(2)} = i\frac{(\omega + d_3)(\omega + d_3 + ig_1\kappa) + i\kappa[g_1(\omega + d_2) + i\kappa]}{D^2}\frac{\partial F}{\partial t_1}e^{i\theta}, \quad (8b)$$

$$A_3^{(2)} = i\frac{(\omega + d_2)[g_1(\omega + d_2) + i\kappa] + i\kappa(\omega + d_3 + ig_1\kappa)}{D^2}\frac{\partial F}{\partial t_1}e^{i\theta}, \quad (8c)$$

$$\Omega_p^{(2)} = 0, \quad (8d)$$

where $\bar{\alpha} = 2\varepsilon^{-2}\text{Im }K(\omega)$.

At the third order ($n = 3$), the condition of eliminating secular term results in the NLS equation with complex coefficients for F,

$$i\frac{\partial F}{\partial z_2} - \frac{1}{2}K_2\frac{\partial^2 F}{\partial t_1^2} - W|F|^2 Fe^{-\bar{\alpha}z_2} = 0 \quad (9)$$

with

$$W = -B\frac{[(\omega + d_3) + |g_1|^2(\omega + d_2) + i\kappa(g_1 + g_1^*)]}{|D|^2 D}$$

$$\times[|\omega + d_3 + i\kappa g_1|^2 + |g_1(\omega + d_2) + i\kappa|^2]. \quad (10)$$

The third-order solution reads

$$A_1^{(3)} = i\left(\alpha_1 F^*\frac{\partial F}{\partial t_1} - \alpha_1^* F\frac{\partial F^*}{\partial t_1}\right)e^{-\bar{\alpha}z_2}, \quad (11a)$$

$$A_2^{(3)} = \left(\alpha_2^{(1)}\frac{\partial^2 F}{\partial t_1^2} + \alpha_2^{(2)}|F|^2 F\right)e^{i\theta}, \quad (11b)$$

$$A_3^{(3)} = \left(\alpha_3^{(1)}\frac{\partial^2 F}{\partial t_1^2} + \alpha_3^{(2)}|F|^2 F\right)e^{i\theta}, \quad (11c)$$

$$\Omega_p^{(3)} = 0, \quad (11d)$$

where the coefficients α_1, $\alpha_2^{(1)}$, $\alpha_2^{(2)}$, $\alpha_3^{(1)}$, and $\alpha_3^{(2)}$ are given in Appendix.

We note that Eq. (9) was also obtained by the method of multiple scales for atomic EIT systems.[5] In that system such equation is enough to give a suitable description of solitons because the probe pulse used in atomic systems has a long-time length (typically around 10^{-6} s). However, as we shall

show below, for the present system the probe pulse has much shorter time length (e.g., around 10^{-12} s), which is necessary for obtaining a nonadiabatic, coherent excitation because the decay rates of quantum-well levels are much larger than those of atomic systems. Accordingly, Eq. (9) is generally invalid for the soliton excitations in the present quantum-well system. Thus we have to go beyond the NLS description by considering next-order approximations.

Using the above solutions from the first to third orders we can solve the fourth-order equations. After a detailed calculation we obtain the condition of eliminating secular term

$$i\frac{\partial F}{\partial z_3} - i\frac{K_3}{6}\frac{\partial^3 F}{\partial t_1^3} - i\beta_1 e^{-\bar{\alpha}z_2}\frac{\partial}{\partial t_1}(|F|^2 F) + i\beta_2 e^{-\bar{\alpha}z_2}F\frac{\partial}{\partial t_1}(|F|^2) = 0,$$
(12)

where coefficients β_1 and β_2 are also given in Appendix.

Combining Eqs. (7), (9), and (12) we obtain a high-order NLS equation with complex coefficients after returning to original variables,

$$i\frac{\partial U}{\partial z} + i\frac{\alpha}{2}U - \frac{K_2}{2}\frac{\partial^2 U}{\partial \tau^2} - i\frac{K_3}{6}\frac{\partial^3 U}{\partial \tau^3} - W|U|^2 U - i\beta_1\frac{\partial}{\partial \tau}(|U|^2 U)$$

$$+ i\beta_2 U\frac{\partial}{\partial \tau}(|U|^2) = 0,$$
(13)

where $\tau = t - z/V_g$ and $U = \varepsilon F e^{-i\alpha z/2}$.

IV. ULTRASLOW OPTICAL SOLITONS

A. A preliminary discussion of Eq. (13)

Equation (13) is a high-order Ginzburg-Landau equation,[48] which has complex coefficients and thus generally does not allows soliton solutions. However, if a practical set of system parameters can be found so that the imaginary part of these coefficients can be made much smaller than their corresponding real part, it can be approximated as a high-order nonlinear NLS equation. Thus it is possible to obtain a shape-preserving soliton solution that can propagate for a rather long distance without significant distortion. This is just the case for the present system when working in the normal dispersion regime, i.e., within the TIT transparency window.

To demonstrate this point we consider a multiple quantum-well structure grown by molecular-beam epitaxial with 200 periods of double quantum wells and sandwiched between 350 nm top and 579 nm bottom contact layer.[49–51] Each double quantum well consists of a narrow well with width of 35 ML and a wide well with width of 51 ML, separated by a 9 ML $Al_{0.2}Ga_{0.8}As$ barriers. The ML in the wide and narrow wells is made by GaAs material with two-dimensional electronic density 10^{11} cm^{-2} and has thickness of 2.83 Å. Double quantum wells are isolated each other by 200 Å wide $Al_{0.2}Ga_{0.8}As$ buffer layers. The energy spacing $E_2 - E_1$ is about 1.67 eV to allow the interband optical excitation by a near-infrared laser with angular frequency $\omega_p = 2.537 \times 10^{15}$ rad/s and the wavelength $\lambda_p = 0.743$ μm. For such system one can use a set of experimentally achievable parameters given by[38,47] $\gamma_{2l} = 1.28$ ns^{-1}, $\gamma_{3l} = 1.29$ ns^{-1},

$\gamma_2^{\text{dph}} = \frac{1}{8}$ ps^{-1}, $\gamma_3^{\text{dph}} = \frac{1}{8}$ ps^{-1}. We take $|g_1| = 0.6$, $B = 6.2 \times 10^5$ m^{-1} meV, $\omega_s = 9.96$ meV, and $\delta = -0.5 \times 10^{12}$ s^{-1}. With these parameters we obtain the values of the coefficients of the high-order NLS Eq. (13) as follows:

$$K_0 = (-1.69 + i0.38) \times 10^3 \text{ cm}^{-1},$$

$$K_1 = (3.01 - i0.65) \times 10^{-9} \text{ cm}^{-1} \text{ s},$$

$$K_2 = (-6.88 + i1.08) \times 10^{-21} \text{ cm}^{-1} \text{ s}^2,$$

$$K_3 = (2.70 - i0.16) \times 10^{-32} \text{ cm}^{-1} \text{ s}^3,$$

$$W = (-3.56 + i0.80) \times 10^{-21} \text{ cm}^{-1} \text{ s}^2,$$

$$\beta_1 = (1.52 - i0.30) \times 10^{-32} \text{ cm}^{-1} \text{ s}^3,$$

$$\beta_2 = (1.67 + i0.41) \times 10^{-32} \text{ cm}^{-1} \text{ s}^3.$$

We see that the imaginary part of these coefficients are indeed much smaller than their corresponding real part. After neglecting the small imaginary part, which can be taken as a perturbation and will be considered in later numerical simulation, Eq. (13) is reduced to the following dimensionless form

$$i\frac{\partial u}{\partial s} + \frac{\partial^2 u}{\partial \sigma^2} + 2u|u|^2$$

$$= i\left[d_0 u + d_1\frac{\partial(|u|^2 u)}{\partial \sigma} + d_2 u\frac{\partial(|u|^2)}{\partial \sigma} + d_3\frac{\partial^3 u}{\partial \sigma^3}\right] + d_4\frac{\partial u}{\partial \sigma},$$
(14)

where we have introduced $s = -z/(2L_D)$, $\sigma = \tau/\tau_0$, $u = U/U_0$, and $d_j = 2L_D/L_j$ ($j = 0-4$), with τ_0 the characteristic time length of the probe pulse, $L_D = \tau_0^2/\widetilde{K}_2$ the characteristic dispersion length, $L_0 \equiv L_A = 2/\alpha$ the characteristic absorption length, $L_1 = \tau_0/(\widetilde{\beta}_1 U_0^2)$ the characteristic nonlinear dispersion length, $L_2 = \tau_0/(\widetilde{\beta}_2 U_0^2)$ the characteristic delay length in nonlinear refractive index, $L_3 = 6\tau_0^3/\widetilde{K}_3$ the characteristic third-order dispersion length, $L_4 = \tau_0/\text{Im } K_1$ the characteristic differential absorption length, and $U_0 = (1/\tau_0)\sqrt{\widetilde{K}_2/\widetilde{W}}$ the characteristic Rabi frequency of the probe field. Here, the quantity with tilde mean its real part, e.g., $\widetilde{K}_2 \equiv \text{Re } K_2$. Notice that in order to form soliton the characteristic Rabi frequency U_0 has been obtained by setting $L_D = L_{NL}$, where L_{NL} is the characteristic nonlinearity length defined by $L_{NL} = 1/(\widetilde{W}U_0^2)$.

Notice that each term in Eq. (14) has clear physical meaning. The second and the third terms on the left-hand side describe, respectively, the second-order dispersion and Kerr nonlinearity of the system. The terms from the first to the fourth ones in the square bracket on the right-hand side describe linear absorption (proportional to d_0), nonlinear dispersion (proportional to d_1), delay response of nonlinear refractive index (proportional to d_2), and third-order dispersion (proportional to d_3), respectively. The last term describes differential absorption (proportional to d_4). If all d_j's ($j = 0-4$)
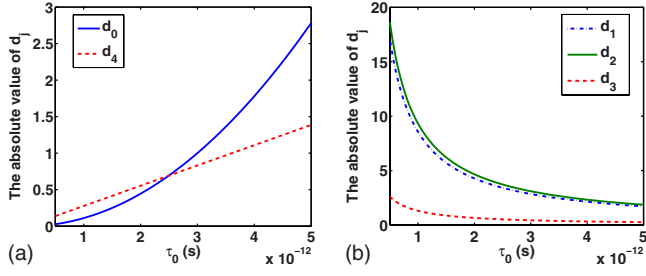
FIG. 3. (Color online) The absolute value of the coefficients d_0, d_4 [panel (a)], and d_1, d_2, d_3 [panel (b)] of Eq. (14) as function of the pulse length τ_0. Both panels (a) and (b) are plotted by the parameters given in Sec. IV.

are zero, Eq. (14) becomes an integrable NLS equation, widely studied in soliton theory.[1,2]

B. Soliton solutions of Eq. (14)

The property of the solution of Eq. (14) is determined by coefficients d_j ($j=0-4$). Using the parameters specified in Sec. IV A we have calculated the values of d_j ($j=0-4$) as functions of the pulse length τ_0 of the probe field, which is shown in Fig. 3. We see that d_3 and d_4 are not sensitive to τ_0. However, d_0, d_1, and d_2 change rapidly as τ_0 varies. Based on the result of Figs. 3(a) and 3(b) we can divide the Eq. (14) into several regimes and hence obtain different soliton solutions, which are given as follows: (1) if $\tau_0 \geq 5.0 \times 10^{-12}$ s, d_1, d_2, d_3, and d_4 are much smaller than d_0 and hence can be neglected. In this case Eq. (14) is reduced to the perturbed NLS equation

$$i\frac{\partial u}{\partial s} + \frac{\partial^2 u}{\partial \sigma^2} + 2u|u|^2 = id_0 u, \qquad (15)$$

The single-soliton solution of this equation can be obtained approximately. The Rabi frequency of the probe field corresponding to such soliton, after returning to original variables, reads[5]

$$\Omega_p = \frac{e^{-d_0 z/L_D}}{\tau_0} \sqrt{\frac{\widetilde{K}_2}{\widetilde{W}}} \mathrm{sech}\left[\frac{e^{-d_0 z/L_D}}{\tau_0}\left(t - \frac{z}{\widetilde{V}_g}\right)\right]$$

$$\times \exp\left[i\widetilde{K}_0 z - i\frac{1 - e^{-2d_0 z/L_D}}{4d_0}\right]. \qquad (16)$$

If $d_0 = 0$, it is an envelope soliton of integrable NLS equation. However, in the case of nonvanishing d_0 the soliton displays a decay of amplitude and an increase in spatial width. However, linear absorption (i.e., nonvanishing d_0) has no effect on the propagating velocity of the soliton. (2) If $\tau_0 \leq 2 \times 10^{-12}$ s, d_0 and d_4 are much smaller than d_1, d_2, and d_3. Thus Eq. (14) in this case is simplified into

$$i\frac{\partial u}{\partial s} + \frac{\partial^2 u}{\partial \sigma^2} + 2u|u|^2 = i\left[d_1\frac{\partial(|u|^2 u)}{\partial \sigma} + d_2 u\frac{\partial(|u|^2)}{\partial \sigma} + d_3\frac{\partial^3 u}{\partial \sigma^3}\right]. \qquad (17)$$

This equation admits exact soliton solutions.[52–54] Hence we obtain the Rabi frequency of the probe field

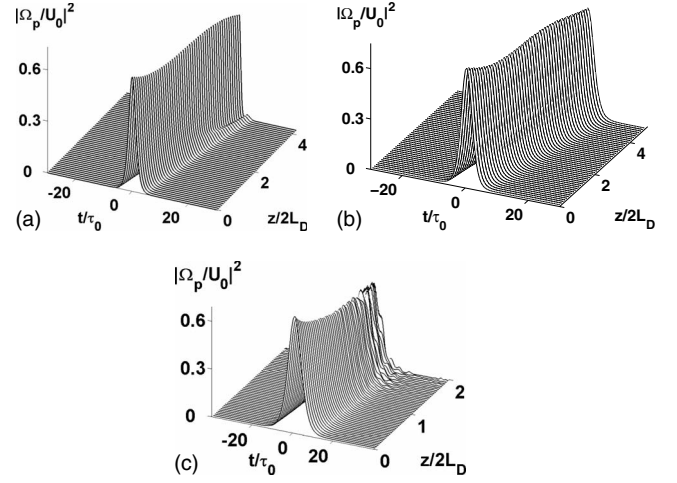

FIG. 4. Soliton wave shape of $|\Omega_p/U_0|^2$ as a function of t/τ_0 and $z/2L_D$. Panel (a): numerical result based on Eqs. (1) and (3) for $\tau_0 = 0.7 \times 10^{-12}$ s and when the soliton propagates to $z=8L_D$ (L_D is dispersion length). Panel (b): numerical result based on Eq. (14) for $\tau_0 = 0.7 \times 10^{-12}$ s and when the soliton propagates to $z=8L_D$. Panel (c): soliton solution based on Eq. (14) with $\tau_0 = 2 \times 10^{-12}$ s. In all numerical simulations the soliton solution (18) has been taken as an initial condition.

$$\Omega_p = U_0 \sqrt{\frac{3(\beta + 3q^2 - 2q)}{d_3^2(3c_1 + c_2)}} \mathrm{sech}\left[\frac{\sqrt{\beta + 3q^2 - 2q}}{d_3}\right.$$

$$\left.\times\left(\frac{t - z/\widetilde{V}_g}{\tau_0} + \frac{\beta z}{2d_3 L_D}\right)\right] \exp\left(i[q^3 - q^2 + (\beta + 3q^2 - 2q)\right.$$

$$\left.\times(1 - 3q)]\frac{z}{2d_3^2 L_D} - i\frac{q}{d_3}\frac{t - z/\widetilde{V}_g}{\tau_0} + i\widetilde{K}_0 z\right) \qquad (18)$$

with the conditions $\beta + 3q^2 - 2q > 0$ and $q \neq 1/3$, where β is a free real number, $c_1 = d_1/(2d_3)$, $c_2 = d_2/(2d_3)$, and $q = (3c_1 + 2c_2 - 3)/[6(c_1 + c_2)]$. Shown in the panel (a) of Fig. 4 is the numerical result of soliton wave shape $|\Omega_p/U_0|^2$ based on Eqs. (1) and (3) for $\tau_0 = 0.7 \times 10^{-12}$ s by taking the soliton solution (18) as initial condition. The other system parameters used are the same as those given in Sec. IV A. We see that soliton is fairly stable when propagating to $z=8L_D$. In the initial stage, the amplitude of the soliton decreases. However, the amplitude increases when propagating to a larger distance and then follows a decrease. At the same time a small radiation appears on one of two wings of the soliton. The physical reason of such behavior is due to the joint contribution from the effects by linear and differential absorption, third-order dispersion and nonlinear dispersion.

For testing the above approximated analytical solutions, the panel (b) of Fig. 4 shows the result of the numerical simulation based on Eq. (14) by using the initial condition the same as that used in panel (a). We see that in this case the soliton is more stable when propagating to $z=8L_D$. The reason is in this case there is exact balance between high-order dispersion and high-order nonlinearity in Eq. (17). (3) When $2 \times 10^{-12} \leq \tau_0 \leq 5 \times 10^{-12}$ s, all d_j's ($j=0-4$) have the same order of magnitude. In this case, one must solve solution of

Eq. (14) numerically. The panel (c) of Fig. 4 shows the result of the numerical simulation based on Eq. (14) with $\tau_0 = 2 \times 10^{-12}$ s by using the initial condition the same as that used in panel (a). We see that in this case the soliton is less stable than the cases of panels (a) and (b). When $z > 3L_D$, the soliton distorts significantly and radiates a lot of small-amplitude continuous waves. This is easy to understand because in this case the high-order dispersion effect and high-order nonlinear effect of the system take significant roles but they cannot balance each other for large propagation distance and time.

We stress that for atomic EIT systems a parameter region where all d_j's can be neglected exists, and hence a description by a simple NLS model is possible.[4,5,8] However, in the present quantum-well system such region does not exist and thus a description by modified NLS equation or high-order NLS equation is necessary.

We now estimate the propagating velocity of the solitons presented above. Using the parameters specified in Sec. IV A we obtain the propagating velocity of the soliton, Eq. (16), as $\widetilde{V}_g = 1.0 \times 10^{-2} c$ for $\tau_0 = 0.7 \times 10^{-12}$ s. The propagating velocity $\widetilde{V}_H$ of the soliton, Eq. (18), is determined by

$$\frac{1}{\widetilde{V}_g^H} = \frac{1}{\widetilde{V}_g} - \frac{\beta\tau_0}{2L_D d_3}. \quad (19)$$

We get $\widetilde{V}_g^H = 1.47 \times 10^{-2} c$ for $\tau_0 = 0.7 \times 10^{-12}$ s and $\beta = 0.5$. We see that the optical solitons predicted here have very slow propagating velocity comparing with the light speed in vacuum.

It is easy to calculate the threshold optical power density required to generate the ultraslow optical solitons given above. The energy flux of the probe filed is given by Poynting's vector integrated over the cross section of the quantum-well sample, i.e., $P = \int dS(\boldsymbol{E}_p \times \boldsymbol{H}_p) \cdot \boldsymbol{e}_z$, where $\boldsymbol{e}_z$ is the unit vector in the propagation direction. Using $\boldsymbol{E}_p = (E_p, 0, 0)$, $\boldsymbol{H}_p = (0, \varepsilon_0 c n_p E_p, 0)$ ($n_p = 1 + c$ Re K/ω_p is the refractive index), and $E_p = (\hbar/|\boldsymbol{\mu}_{12}|)\Omega_p \exp[i(k_p z - \omega_p t)] + $c.c., we can get the expressions of P for different soliton solutions. Then the integration of P over a carrier-wave period gives the average energy flux of the probe field, i.e.,

$$\bar{P} = \bar{P}_{max,1} \operatorname{sech}^2\left[\frac{1}{\tau_0}\left(t - \frac{z}{\widetilde{V}_g}\right)\right], \quad \text{[for the soliton(16)]}, \quad (20a)$$

$$\bar{P} = \bar{P}_{max,2} \times \operatorname{sech}^2\left[\frac{\sqrt{\beta + 3q^2 - 2q}}{d_3\tau_0} \times \left(t - \frac{z}{\widetilde{V}_g^H}\right)\right], \quad \text{[for the soliton(18)]} \quad (20b)$$

with corresponding peak powers

$$\bar{P}_{max,1} \approx 2\varepsilon_0 c n_p S_0\left(\frac{\hbar}{|\boldsymbol{\mu}_{12}|}\right)^2 \frac{1}{\tau_0^2} \frac{\widetilde{K}_2}{\widetilde{W}}, \quad (21a)$$

$$\bar{P}_{max,2} \approx \varepsilon_0 c n_p S_0\left(\frac{\hbar}{|\boldsymbol{\mu}_{12}|}\right)^2 \frac{6(\beta + 3q^2 - 2q)}{d_3^2\tau_0^2(3c_1 + 2c_2)} \frac{\widetilde{K}_2}{\widetilde{W}}, \quad (21b)$$

where $S_0 = \pi R^2$ is the cross-section area of the probe laser beam. Using the above numerical values of system parameters and take $|\boldsymbol{\mu}_{12}| = 2.688 \times 10^{-28}$ mC and $S_0 = \pi \times 10^{-7}$ cm^2 we obtain $\bar{P}_{max,1} = 41.50$ mW and $\bar{P}_{max,2} = 63.12$ mW, respectively. Thus, only very low input power is needed for generating the ultraslow optical solitons in the semiconductor multiple quantum-well structure.

C. Discussion on validity conditions of SVEA

Recall that SVEA condition, Eq. (2), has been used for obtaining Eq. (3) governing the evolution of the Rabi frequency Ω_p of the probe field. In the case of the soliton solutions given above, such condition corresponds to

$$\lambda_p \ll \widetilde{V}_g\tau_0, \quad (22a)$$

$$\omega_p\tau_0 \gg 1. \quad (22b)$$

It is easy to check that the soliton solutions presented above satisfy these conditions. In fact, by using the system parameters specified in Sec. IV A, we have $\lambda_p = 0.743$ μm, $\omega_p = 2.537 \times 10^{15}$ rad s^{-1}, and $\widetilde{V}_g = 1.0 \times 10^{-2} c$. Since $\tau_0 = 0.7 \times 10^{-12}$ s, we obtain $\widetilde{V}_g\tau_0 = 2.11$ μm and $\omega_p\tau_0 = 1.776 \times 10^3$, which validate fairly well the SVEA condition (22).

In order to make a low-light soliton generated effectively and propagate stably in the quantum-well system, additional requirement

$$L_D = L_{NL} \leq L, \quad (23a)$$

$$L_D \leq L_A, \quad (23b)$$

$$L_{sol} \leq L, \quad (23c)$$

should also be fulfilled, where $L_{sol} \equiv \widetilde{V}_g\tau_0$ is the spatial length of the soliton and L is the length of the multiple quantum-well structure. In our system

$$L = [51 \times 2.83 \text{ Å(wide well thickness)} + 9 \\ \times 2.83 \text{ Å(barrier thickness)} + 35 \\ \times 2.83 \text{ Å(narrow well thickness)} \\ + 200 \text{ Å(buffer layer thickness)} \times 200(\text{period}) \\ = 9.377 \ \mu\text{m},$$

the probe-field time length τ_0 is chosen as the order of picosecond, we have $L_{sol} = 2.11$ μm, $L_D = 0.71$ μm, $L = 9.377$ μm, and $L_A = 26.12$ μm. Thus the requirement, Eq. (23), can also be satisfied. We stress that the interband transition scheme adopted in the present study, which makes the probe wavelength λ_p is in near-infrared (visible) region, is crucial for satisfying the SVEA condition (22) and the additional requirement, Eq. (23), listed above.

However, if adopting an intersubband transition the SVEA condition is hard to be satisfied. The main reason is

that the probe wavelength λ_p is too long (about 10 μm or larger) and probe pulse length τ_0 cannot be too big due to the constraint from large energy-level decay rates of quantum-well systems. Recently, slow-light solitons have been suggested by the authors of Refs. 40 and 41 based on intersubband transition scheme. Unfortunately, the calculation in those works violate either the SVEA condition (22) or the additional requirement, Eq. (23), and hence the scheme adopted is unrealistic in physics.

V. SUMMARY

We have investigated the formation and propagation of optical solitons in an asymmetric double quantum-well structure. By using a standard method of multiple scales we have derived a high-order nonlinear NLS equation, which includes effects of linear and differential absorption, nonlinear dispersion, delay response of nonlinear refractive index, and third-order dispersion of the probe field. We have shown that, in order to make slowly varying envelope approximation be valid, an excitation scheme of interband transition should be adopted. We have also shown that for realistic quantum-well parameters the probe field with time length of picosecond or shorter must be used to make dispersion and nonlinear lengths of the system be smaller than absorption length, only under such conditions a shape-preserving propagation of optical solitons is available. In addition, we have clarified the validity domain for the perturbed NLS equation as well as the high-order NLS equation and provide various optical soliton solutions in different regimes. We have demonstrated that the solitons obtained have ultraslow propagating velocity and can be generated under very low input light intensity. The results presented in this work may be useful for the experimental generation of ultraslow optical solitons in multiple quantum-well systems and useful for the application of optical information processing and transmission.

ACKNOWLEDGMENTS

APPENDIX

Expressions of α_1, $\alpha_2^{(1)}$, $\alpha_2^{(2)}$, $\alpha_3^{(1)}$, and $\alpha_3^{(2)}$ in Eq. (11) are given by

$$\alpha_1 = \frac{|\omega + d_3|^2(\omega + d_3) + |g_1(\omega + d_2)|^2(\omega + d_2) + i\kappa q + \kappa^2 R}{2|D|^2 D^*},$$
(A1)

$$\alpha_2^{(1)} = \frac{(\omega + d_3)^3 + i\kappa g_1 Q - \kappa^2(3\omega + 2d_3 + d_2) - i\kappa^3 g_1}{D^3},$$
(A2)

$$\alpha_2^{(2)} = -\frac{W(\omega + d_3 + i\kappa g_1)}{2B\Omega},$$
(A3)

$$\alpha_3^{(1)} = \frac{g_1(\omega + d_2)^3 + i\kappa Q - \kappa^2 g_1(3\omega + 2d_2 + d_3) - i\kappa^3}{D^3},$$
(A4)

$$\alpha_3^{(2)} = -\frac{W[g_1(\omega + d_2) + i\kappa]}{2B\Omega}$$
(A5)

with $R = |g_1|^2(\omega + d_2) + (\omega + d_3) - \Omega^*$ and $Q = (\omega + d_2)^2 + (\omega + d_2)(\omega + d_3) + (\omega + d_3)^2$.

Expressions of β_1 and β_2 in Eq. (12) read

$$\beta_1 = \frac{2B\Omega}{D}(\alpha_1 + \alpha_1^*) - \left(\frac{1}{V_g} - \frac{1}{c}\right)\frac{WD}{B\Omega},$$
(A6)

$$\beta_2 = \frac{2B\Omega}{D}(\alpha_1 + 2\alpha_1^*) - \frac{1}{2}\left(\frac{1}{V_g} - \frac{1}{c}\right)\frac{WD}{B\Omega},$$
(A7)

where $q = g_1(\omega + d_2)(\omega + d_3^*) + \text{c.c.}$ and $\Omega = (\omega + d_3) + |g_1|^2(\omega + d_2) + i\kappa(g_1 + g_1^*)$.

*gxhuang@phy.ecnu.edu.cn

[1] Y. S. Kivshar and G. P. Agrawal, *Optical Solitons: From Fibers to Photonic Crystals* (Academic, San Diego, 2003).

[2] A. Hasegawa and M. Matsumoto, *Optical Solitons in Fibers* (Springer, Berlin, 2003).

[3] M. Fleischhauer, A. Imamoglu, and J. P. Marangos, Rev. Mod. Phys. **77**, 633 (2005), and references therein.

[4] Y. Wu and L. Deng, Phys. Rev. Lett. **93**, 143904 (2004).

[5] G. Huang, L. Deng, and M. G. Payne, Phys. Rev. E **72**, 016617 (2005).

[6] L. Deng, M. G. Payne, G. Huang, and E. W. Hagley, Phys. Rev. E **72**, 055601(R) (2005).

[7] G. Huang, K. Jiang, M. G. Payne, and L. Deng, Phys. Rev. E **73**, 056606 (2006).

[8] C. Hang, G. Huang, and L. Deng, Phys. Rev. E **73**, 036607 (2006).

[9] C. Hang and G. Huang, Phys. Rev. A **77**, 033830 (2008).

[10] A. Imamōglu and R. J. Ram, Opt. Lett. **19**, 1744 (1994).

[11] D. E. Nikonov, A. Imamoğlu, and M. O. Scully, Phys. Rev. B **59**, 12212 (1999).

[12] C. R. Lee, Y. C. Li, F. K. Men, C. H. Pao, Y. C. Tsai, and J. F. Wang, Appl. Phys. Lett. **86**, 201112 (2005).

[13] M. D. Frogley, J. F. Dynes, M. Beck, J. Faist, and C. C. Phillips, Nature Mater. **5**, 175 (2006).

[14] H. Wang, M. Jiang, and D. G. Steel, Phys. Rev. Lett. **65**, 1255 (1990).

[15] J. F. Dynes, M. D. Frogley, J. Rodger, and C. C. Phillips, Phys. Rev. B **72**, 085323 (2005).

[16] M. Phillips and H. Wang, Phys. Rev. Lett. **89**, 186401 (2002).

[17] M. Phillips and H. Wang, Opt. Lett. **28**, 831 (2003).

[18] M. C. Phillips, H. Wang, I. Rumyantsev, N. H. Kwong, R. Takayama, and R. Binder, Phys. Rev. Lett. **91**, 183602 (2003).

[19] P. C. Ku, C. J. Chang-Hasnian, and S. L. Chuang, Electron. Lett. **38**, 1581 (2002).

[20] P. C. Ku, F. Sedgwick, C. J. Chang-Hasnain, P. Palinginis, T. Li, H. Wang, S.-W. Chang, and S.-L. Chuang, Opt. Lett. **29**, 2291 (2004).

[21] P. Palinginis, S. Crankshaw, F. Sedgwick, E.-T. Kim, M. Moewe, C. J. Chang-Hasnain, H. Wang, and S.-L. Chuang, Appl. Phys. Lett. **87**, 171102 (2005).

[22] H. Su and S.-L. Chuang, Appl. Phys. Lett. **88**, 061102 (2006).

[23] H. Su and S.-L. Chuang, Opt. Lett. **31**, 271 (2006).

[24] S. Sarkar, Y. Guo, and H. Wang, Opt. Express **14**, 2845 (2006).

[25] P. C. Ku, C. J. Chang-Hasnain, and S.-L. Chuang, J. Phys. D **40**, R93 (2007), and references therein.

[26] K. Maschke, P. Thomas, and E. O. Góbel, Phys. Rev. Lett. **67**, 2646 (1991).

[27] J. Faist, F. Capasso, A. L. Hutchinson, L. Pfeiffer, and K. W. West, Phys. Rev. Lett. **71**, 3573 (1993).

[28] J. Faist, C. Sirtori, F. Capasso, S.-N. Chu, L. N. Pfeiffer, and K. W. West, Opt. Lett. **21**, 985 (1996).

[29] J. Faist, F. Capasso, C. Sirtori, A. L. Hutchinson, K. W. West, and L. N. Pfeiffer, Appl. Phys. Lett. **71**, 3477 (1997).

[30] H. Schmidt, K. L. Campman, A. C. Gossard, and A. Imamoglu, Appl. Phys. Lett. **70**, 3455 (1997).

[31] L. Silvestri, F. Bassani, G. Czajkowski, and B. Davoudi, Eur. Phys. J. B **27**, 89 (2002).

[32] S. F. Yelin and P. R. Hemmer, Phys. Rev. A **66**, 013803 (2002).

[33] P. Ginzburg and M. Orenstein, Opt. Express **14**, 12467 (2006).

[34] H. Schmidt and A. Imamoglu, Opt. Commun. **131**, 333 (1996).

[35] H. Sun, S. Gong, Y. Niu, S. Jin, R. Li, and Z. Xu, Phys. Rev. B **74**, 155314 (2006).

[36] H. Sun, Y. Niu, R. Li, S. Jin, and S. Gong, Opt. Lett. **32**, 2475 (2007).

[37] J. H. Wu, J. Y. Gao, J. H. Xu, L. Silvestri, M. Artoni, G. C. La Rocca, and F. Bassani, Phys. Rev. Lett. **95**, 057401 (2005).

[38] Y. Xue, X.-M. Su, G. W. Wang, Y. Chen, and J.-Y. Gao, Opt. Commun. **249**, 231 (2005).

[39] X. Hao, J. Li, J. Liu, P. Song, and X. Yang, Phys. Lett. A **372**, 2509 (2008).

[40] W.-X. Yang, J.-M. Hou, and R.-K. Lee, Phys. Rev. A **77**, 033838 (2008).

[41] W.-X. Yang and R.-K. Lee, EPL **83**, 14002 (2008).

[42] H. G. Roskos, M. C. Nuss, J. Shah, K. Leo, D. A. B. Miller, A. M. Fox, S. Schmitt-Rink, and K. Köhler, Phys. Rev. Lett. **68**, 2216 (1992).

[43] I. Waldmüller, J. Förstner, S.-C. Lee, A. Knorr, M. Woerner, K. Reimann, R. A. Kaindl, T. Elsaesser, R. Hey, and K. H. Ploog, Phys. Rev. B **69**, 205307 (2004).

[44] *Quantum Well Intersubband Transition Physics and Devices*, edited by C. Liu, B. F. Levine, and J. Y. Andersson, (Kluwer Academic, Netherlands, 1994).

[45] S. E. Harris, Phys. Rev. Lett. **62**, 1033 (1989).

[46] A. Imamoğlu, Phys. Rev. A **40**, 2835 (1989).

[47] A. Neogi, Opt. Commun. **133**, 479 (1997); A. Neogi, H. Yoshida, T. Mozume, and O. Wada, *ibid.* **159**, 225 (1999); A. Neogi, O. Wada, Y. Takahashi, and H. Kawaguchi, Opt. Lett. **23**, 1212 (1998).

[48] A. C. Newell and J. V. Moloney, *Nonlinear Optics* (Addison-Wesley, Redwood City, CA, 1992), Chap. 6.

[49] F. Szmulowicz, G. J. Brown, H. C. Liu, A. Shen, Z. R. Wasilewski, and M. Buchanan, Opto-Electron. Rev. **9**, 164 (2001).

[50] C. A. C. Endocarp and T. H. Chic, IEEE Explore. **21-25**, 549 (1996).

[51] K. L. Vodopyanov, K. O'Neill, G. B. Serapiglia, C. C. Phillips, M. Hopkinson, I. Vurgaftman, and J. R. Meyer, Appl. Phys. Lett. **72**, 2654 (1998).

[52] M. Gedalin, T. C. Scott, and Y. B. Band, Phys. Rev. Lett. **78**, 448 (1997).

[53] K. Nakkeeran, K. Porsezian, P. S. Sundaram, and A. Mahalingam, Phys. Rev. Lett. **80**, 1425 (1998).

[54] S. L. Palacios, A. Guinea, J. M. Fernandez-Diaz, and R. D. Crespo, Phys. Rev. E **60**, R45 (1999).